

Collective electronic excitations in metal coated C₆₀

A. Rubio*

*Department of Physics, University of California at Berkeley, Berkeley, California 94720
and Materials Sciences Division, Lawrence Berkeley Laboratory, Berkeley, California 94720*

J. A. Alonso, J. M. López and M. J. Stott†

*Departamento de Física Teórica, Universidad de Valladolid, E-47011 Valladolid, Spain
(Received 16 December 1993; revised manuscript received 8 March 1994)*

A two-shell jellium-on-jellium model has been used to study the collective electronic excitations of C₆₀ coated by an increasing number N of Na atoms. We predict a transition from the π -electron polarization of the fullerene to the metallic sodium polarization as a function of increasing N . For low coverages, the Na layer produces only a broadening and fragmentation of the π plasmon of C₆₀. However, if the coverage is large enough, a Na surface plasmon appears. This occurs only after the electron density of the cluster clearly shows two distinct regions, the outer one having an "average" density similar to that in pure Na metal or Na clusters. The induced density at the collective-mode frequency shows structure corresponding to two interfaces, C₆₀-Na and Na vacuum, the first peak becoming less pronounced as the coverage increases due to a transfer of oscillator strength to the metallic counterpart. The static polarizability per electron also shows this trend and tends slowly to the Na value from below after an initial sharp rise in the region $N \sim 13$ -21.

I. INTRODUCTION

The discovery of the C₆₀ molecule¹ has been followed by the synthesis of a solid material with face-centered-cubic structure in which the C₆₀ units retain their identity.² After doping with alkali-metal atoms in the adequate proportion, this solid shows superconducting properties.³ More recently, C₆₀ molecules have been condensed into finite (C₆₀) _{n} clusters⁴ which appear to grow following an icosahedral pattern, similar to clusters of the inert gases.⁵ Martin and co-workers⁶ have coated the surface of the (C₆₀) _{n} clusters with alkali atoms (Li, Na, K) and the mass spectra of the positively ionized coated clusters, as a function of the number of coating atoms, shows interesting features not yet explained.

The experimental studies of the electronic properties of C₆₀ in the gas phase⁷ and in the solid form⁸ have shown the presence of two collective excitations, associated with the collective motion of the π and of the σ electrons of C₆₀. The π resonance occurs at about 6 eV and the σ resonance at about 20 eV. Theoretical calculations⁹⁻¹⁶ give results in good agreement with experiment. A great deal of theoretical and experimental work has also been reported on the collective electronic excitations of alkali-metal clusters.¹⁷ The characteristic of these clusters is a surface plasmon at energies ~ 2 -3 eV, that is, 3-4 eV below the energy of the π plasmon of C₆₀. For instance, for Na clusters this plasmon occurs at ~ 2.5 eV. One can ask what would happen to the low energy plasmon of C₆₀ when this cluster becomes coated with increasing amounts of Na. It is reasonable to expect that when C₆₀ is coated with several sodium layers, the Na cluster surface plasmon would become a prominent excitation but the coverage at which this would first appear and the nature of the appearance are points of interest which

remain to be settled. In this paper, we use a simple model for C₆₀ coated with Na and calculate the optical spectrum in order to study the evolution of the collective excitations as a function of Na coverage.

II. CLUSTER MODEL

The collective electronic properties of C₆₀ have been studied using several models and methods.⁹⁻¹⁶ A common characteristic of some of this work^{9,12-15} is the modeling of the positive background, consisting of the nuclei plus core electrons of the cluster, by a shell of uniform charge and finite thickness. This is the so called jellium-shell model. Despite its simplicity the model gives the position of the π plasmon in good overall agreement with experiment and close to that obtained by more accurate methods in which the granularity of the cluster is accounted for.^{9,13} It is well known that the jellium background model also works well for alkali-metal clusters,¹⁷ or surfaces,¹⁸ and that the introduction of lattice effects causes only a minor modification in the calculated optical properties.¹⁹

In this paper, we use a two-shell jellium model to describe (C₆₀Na _{N})⁺ clusters. The inner jellium shell represents the ionic background of the C₆₀ cluster and the outer shell that of the coating metal. The density of the positive background is then

$$\rho_+(r) = \begin{cases} \rho_1, & R - \Delta_1 \leq r \leq R + \Delta_1 \\ \rho_2, & R + \Delta_1 \leq r \leq R + \Delta_1 + \Delta_2 \\ 0, & \text{otherwise.} \end{cases} \quad (1)$$

This means that the C₆₀ shell is bounded by inner and outer radii $R - \Delta_1$ and $R + \Delta_1$, respectively, where

$R=6.64$ a.u. is the observed radius of C_{60} .²⁰ We are primarily interested in the π plasmon of C_{60} because it is in the same energy range as the Na-metallic electronic levels. Consequently, we take each C atom in our model to contribute only one electron to the electronic cloud. The layer thickness $2\Delta_1$ has been chosen equal to 1 a.u. This value leads to a position of the π plasmon of free C_{60} in good agreement with experiment and with more accurate models.¹³ The background density ρ_1 is related to R and Δ_1 by $60 = \frac{4\pi}{3}[(R + \Delta_1)^3 - (R - \Delta_1)^3]\rho_1$. The external layer representing the coating atoms rests directly on the C_{60} shell. Its density ρ_2 has been fixed to be the known density of the bulk Na metal ($\rho_2 = 0.004$ e/a.u.³) and its thickness Δ_2 depends on the number N of coating atoms through the equation

$$N = \frac{4\pi}{3}[(R + \Delta_1 + \Delta_2)^3 - (R + \Delta_1)^3]\rho_2. \quad (2)$$

With this model, the ground state electronic structure of the clusters [that is, the one electron energy eigenvalues, ϵ_i , and the electron density, $\rho(\vec{r})$], can be calculated using the density functional theory (DFT) in its customary Kohn-Sham version²¹. The self-consistent effective potential $V_{\text{eff}}(\vec{r})$ seen by the electrons is the sum of the external potential produced by the ionic background given in Eq. (1), the Hartree potential of the electrons and the exchange-correlation potential. For the last piece we use the local density approximation (LDA). For small numbers of Na atoms adsorbed on C_{60} the experimental mass spectra⁶ show typical small coverage effects, but after seven atoms, the spectra show clear odd-even alternation similar to that observed in the mass spectra of sodium clusters. Consequently, we expect our two-slab model for fullerenes coated by alkali atoms to begin to give a realistic description of the electronic properties for $N \sim 13$, and especially for larger N corresponding to closed shells. The experimental findings for low coverages could correlate with the special electronic properties of sodium intercalation fullerite compounds (Na_6C_{60} shows a conventional ionic structure²²). In the present work, we will not analyze this small coverage limit where a more sophisticated geometrical model is needed; instead we will concentrate on the optical response for large coverages where the two-slab model, as stated before, is more reliable.

III. CALCULATION OF THE COLLECTIVE ELECTRONIC RESPONSE

To calculate the collective response we have used the time-dependent DFT. Since exchange and correlation effects are treated at the LDA level, the method is known as time-dependent LDA.^{23,24} The fundamental ingredient of this theory is the dynamical susceptibility $\chi(\vec{r}_1, \vec{r}_2, \omega)$, which is obtained from a Dyson-type integral equation

$$\chi = \chi_0 + \chi_0 K \chi. \quad (3)$$

Here, χ_0 is the noninteracting susceptibility, which can be constructed from a number of ingredients arising in the ground state Kohn-Sham calculation, and the kernel

K is the functional derivative of the ground state effective potential $K(\vec{r}_1, \vec{r}_2) = \delta V_{\text{eff}}(\vec{r}_1)/\delta \rho(\vec{r}_2)$. The electron density induced by the applied, external, multipolar field, and the corresponding dynamical polarizability, $\alpha(\omega)$, are immediately obtained from χ and the applied field. The static polarizability is given by $\alpha(\omega = 0)$. Finally, the photoabsorption cross section $\sigma(\omega)$ is obtained from

$$\sigma(\omega) = \frac{4\pi\omega}{c} \text{Im}\alpha(\omega). \quad (4)$$

References 13 and 24 can be consulted for details. In what follows, we will present results for the dipolar response of coated carbon clusters, which is readily accessible experimentally through optical measurements.

The physical picture of a certain excitation being single pair, or a collective surface mode, or a strong coupling of all these excitations may be visualized^{25,26} by considering the frequency-dependent induced charge density $\delta n(\vec{r}, \omega)$ defined as

$$\delta n(\vec{r}, \omega) = \int d\vec{r}_1 \chi(\vec{r}, \vec{r}_1, \omega) V_{\text{ext}}(\vec{r}_1, \omega), \quad (5)$$

where $V_{\text{ext}}(\vec{r}, \omega)$ is the frequency-dependent external potential, and analyzing the real and imaginary parts of $\delta n(\vec{r}, \omega)$. However, an unambiguous assignment of a mode as collective requires a more detailed investigation of the origin of the excitation such as that performed by Nuroh et al.²⁷

IV. RESULTS

The electronic structure of C_{60}^+ in the jellium-shell model is $1s(2)$, $1p(6)$, $1d(10)$, $1f(14)$, $1g(18)$, $1h(9)$, where the occupation of the electronic shells is given in parentheses. The least bound occupied shell, $1h$, is only partially filled due to the degeneracy induced by the spherical approximation used in the calculation. The calculated photoabsorption cross section $\sigma(\omega)$ is given in Fig. 1. It shows a collective resonance located at ~ 8 eV. These results and those reported in similar figures were obtained with an artificial broadening of the lines of 0.1 eV in order to simulate finite temperature effects on the photoabsorption cross section.²⁸ The results for neutral C_{60} are rather similar and have been reported in Ref. 13 (in that work, however, the thickness of the C_{60} shell was slightly different, namely, $2\Delta_1 = 0.8$ a.u.). The independent particle response, composed of single-particle excitations, is given by the dashed curve. The collective resonance shows some fragmentation due to the interaction with single-particle transitions which in our LDA approach correspond to bound-continuum transitions because the calculated ionization threshold is 7 eV (peaks below this value in the dashed line are due to bound-bound transitions).

We have studied several $[\text{C}_{60}\text{Na}_N]^+$ clusters with increasing values of N to investigate the modifications of the collective response and its evolution with N . The specific values of N studied are $N=13$, 21, 45, 65, and 93. It should be noted that we have performed our calculations for ionized clusters so as to correspond as closely as

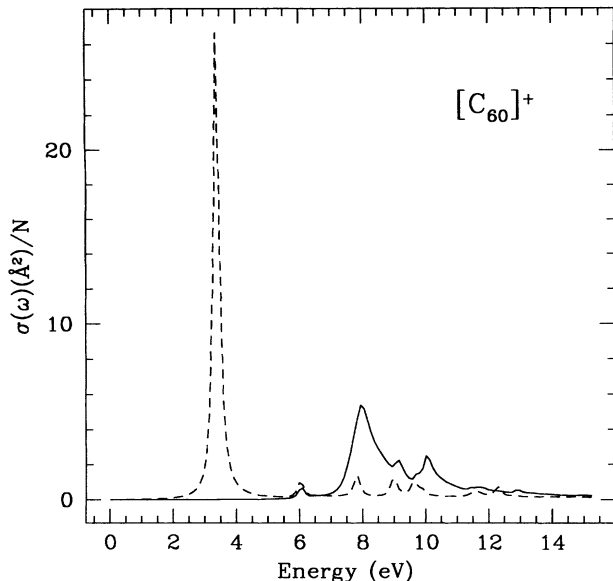


FIG. 1. Calculated photoabsorption cross section per electron for C_{60}^+ (full curve). The cross section calculated from the noninteracting response is given by the dashed curve.

possible with the mass spectra reported by Martin *et al.*⁶ These workers designed their experiments to reveal the relative stability of ionized species. For this purpose, the photoionized clusters were heated with a laser to allow for atom evaporation. Since Na is a monovalent atom, the number of active electrons in these clusters is $60+N-1$. All the clusters studied have closed electronic shells for which the spherical approximation assumed in the response calculations is best justified. The ground state electron densities of some of the clusters are shown in Fig. 2. There is a clear distinction between $N=13, 21$ on the one hand, and $N=45, 65, 93$ on the other. The cases of $N=13, 21$ show electron densities that look rather similar to those of C_{60}^+ or C_{60} (see also Ref. 13). Although the electron density is more extended in $[C_{60}Na_{13}]^+$ and $[C_{60}Na_{21}]^+$, there is still only a single decay length. In

contrast the densities for $N=45, 65,$ and 93 show two decay lengths. This means that the outer surface of the cluster has some resemblance to the surface of pure Na clusters and one can expect, as Ekardt has indicated in his work on metal-on-metal coated particles,²⁹ to observe new features related to the Na surface and volume plasmons. Similar behavior has also been observed in adsorbed alkali-metal layers on metallic surfaces.³⁰

Let us now turn to analyzing the collective response. This is given in Fig. 3 for $[C_{60}Na_{13}]^+$. The thickness of the coating layer is 3.35 a.u. The electrons contributed by the Na layer lead to the complete filling of the $1h$ shell with 22 electrons. The energy gap [highest occupied molecular orbital-lowest unoccupied molecular orbital (HOMO-LUMO) gap] between this electronic shell and the lowest unoccupied shell, which is of $2s$ character, is small (0.18 eV). The binding energies of the occupied shells are smaller with respect to C_{60}^+ due to a more extended and shallower effective potential. The situation is more complex for the unoccupied shells. We find shifts up and down in their binding energies, but all these changes are small. Consequently the single-particle transitions, both bound-bound and bound-unbound occur at lower energies, compared to C_{60}^+ , as can be seen from a comparison of the noninteracting spectra of C_{60}^+ and $[C_{60}Na_{13}]^+$ which are represented by dashed lines in Fig. 1 and 3. The peaks in the single particle spectra are at the transition energies for single particle excitations and the heights are proportional to the oscillator strengths for the modes. The very prominent peak in the noninteracting cross section is due to $1h-1i$ single particle transitions. In fact, this transition gives the dominant peak in the noninteracting spectra for all the cases presented here, although other transitions, e.g., $2h-2i, 1h-2g$, also lead to sizeable peaks for the larger N values shown in Fig. 4. The effect of the Na cladding on the fully interacting photoabsorption spectrum (of $[C_{60}Na_{13}]^+$) is a spreading of the plasmon down to lower energies by more than 1 eV and a reduction in amplitude. This is mainly due to an increased fragmentation of the spectrum because of the interaction of the collective resonance with

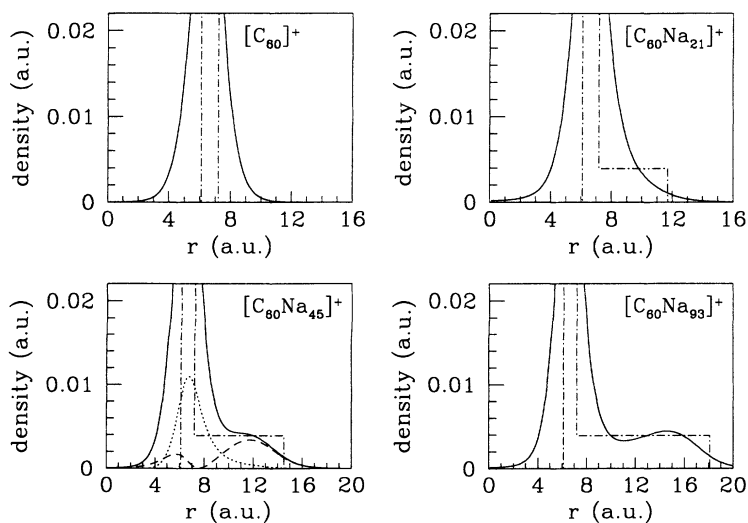


FIG. 2. Electron density and positive background density versus the distance r to the cluster center in the two-slab jellium-on-jellium model of C_{60}^+ , $[C_{60}Na_{21}]^+$, $[C_{60}Na_{45}]^+$ and $[C_{60}Na_{93}]^+$. The maximum of the electron density (not shown in order to enhance the low density features) reaches values $\sim 0.04-0.05$ a.u. Dash-dotted lines represent the background ionic charge density. The plot corresponding to $N=45$ shows partial contributions to the total electron density from the $1h$ charge density (dotted line) and the $2s+2p+2d+2f$ charge density (dashed line) (see main text).

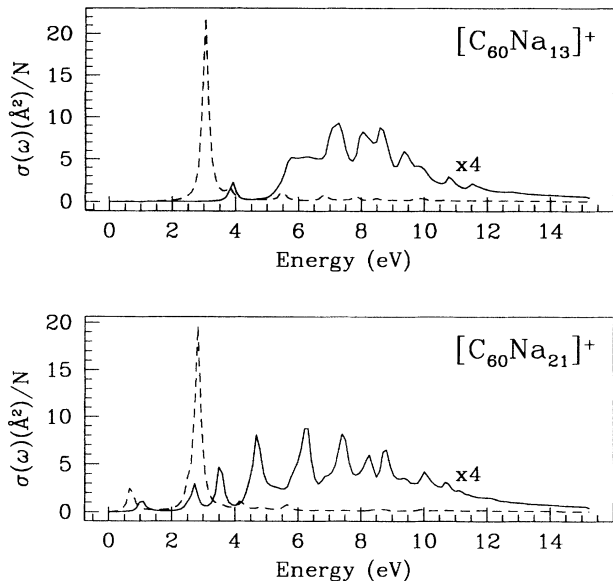


FIG. 3. Calculated photoabsorption cross section, per electron, for $[\text{C}_{60}\text{Na}_{13}]^+$ and $[\text{C}_{60}\text{Na}_{21}]^+$ (full curves). The cross section calculated from the noninteracting response is given by the dashed curves. The interacting response has been multiplied by 4 in order to display the features of the spectrum.

particle-hole transitions (Landau damping).

The ground state electronic configuration of the $[\text{C}_{60}\text{Na}_{21}]^+$ is $1s, 1p, 1d, 1f, 1g, 2s, 2p, 1h$ (all shells completely filled). We notice that the $2s$ and $2p$ levels have dropped below the $1h$ level. The gap between $1h$ and the lowest unoccupied level ($2d$) is equal to 0.61 eV, much larger than the HOMO-LUMO gap in $[\text{C}_{60}\text{Na}_{13}]^+$. This appears to correlate with the fact that $[\text{C}_{60}\text{Na}_{21}]^+$

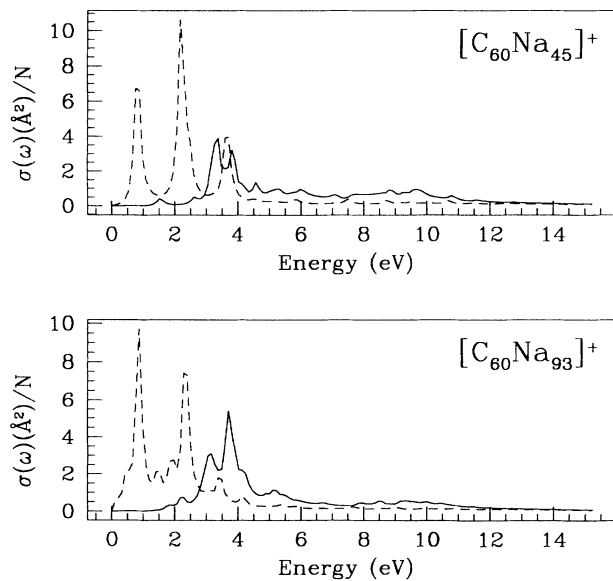


FIG. 4. Calculated photoabsorption cross-section, per electron, of $[\text{C}_{60}\text{Na}_{45}]^+$ and $[\text{C}_{60}\text{Na}_{93}]^+$ (full curves). The cross section calculated from the noninteracting response is given by the dashed curves.

is a magic cluster (high abundance) in the mass spectra of Martin *et al.*⁶ The modified electronic structure leads to new single-particle transitions and to a strongly broadened and fragmented photoabsorption cross section (Fig. 3) with no prominent feature remaining at ~ 8 eV, the position of the C_{60}^+ plasmon mode. Furthermore, some strength begins to appear in the energy region around 2–4 eV, typical of alkali-metal clusters. This indicates the beginning of the transition from the carbon π -electron response to the Na-metallic response.

A drastic change in $\sigma(\omega)$ is observed for $[\text{C}_{60}\text{Na}_{45}]^+$ (see Fig. 4). Its electronic configuration is $1s, 1p, 1d, 1f, 1g, 2s, 2p, 2d, 1h, 2f$. The $2d$ level has also dropped below the $1h$. The electron density of the cluster is composed of two pieces: the innermost electrons are localized in the C_{60} shell; the $2s, 2p, 2d$, and $2f$ electrons can be ascribed to the Na layer, and the $1h$ electrons, which are located near the carbon-sodium interface, are shared by the C_{60} and Na layers. This division is illustrated in the corresponding plot of Fig. 2, where the dotted line gives the $1h$ charge density and the dashed line the $2s+2p+2d+2f$ charge density. The Na layer now shows its identity through the appearance of a strong peak in the photoabsorption spectrum at low energy (~ 3 –3.5 eV). This peak has a broad tail extending to higher energies, and a considerable amount of strength is still concentrated in the region 4–11 eV, typical of the π -carbon absorption spectrum, although the amplitude is further reduced from the clusters with smaller N .

Finally, the largest cluster studied is $[\text{C}_{60}\text{Na}_{93}]^+$; the picture is rather similar to that for $[\text{C}_{60}\text{Na}_{45}]^+$. Now the electronic closed-shell configuration has as occupied levels: $1s, 1p, 1d, 1f, 1g, 2s, 2p, 2d, 2f, 2g, 1h, 3s, 3p, 2h$. The peak at the position of the Na surface plasmon is now well developed (see Fig. 4), and the cluster responds much like a pure ionized Na cluster [the TDLDA surface plasmon of jelliumlike ionized Na clusters occurs at 3–3.5 eV (Ref. 31)]. The collective resonance has a broad tail and some strength is still concentrated in the region 8–10 eV although the response there is much attenuated compared to pure C_{60}^+ .

To get more insight into the shift of the collective resonance from C_{60}^+ to that more typical of sodium clusters as the coating is increased, we have plotted in Fig. 5 the dipolar induced charge density [see Eq. (5)] corresponding to the frequency of the collective mode for C_{60}^+ , $[\text{C}_{60}\text{Na}_{45}]^+$ and $[\text{C}_{60}\text{Na}_{93}]^+$ (that is, 8 eV, 3.4 eV, and 3.7 eV, respectively). Comparing $N=45$ and $N=93$ we observe a partial shift of the induced charge from the carbon-Na interface to the Na-vacuum interface, but it is interesting to see that even in the case of $N=93$ a significant contribution to the induced charge density still occurs at the carbon-Na interface, and complete localization of the induced charge at the Na-vacuum interface, as one would expect for a purely metallic Na response, is incomplete. Clearly both interfaces contribute to the collective electronic motion but only one surface plasmon is observed. Its resonance energy tends to be dominated by the sodium coating.³² Classical electromagnetic arguments give two coupled surface-interface plasmons with both the interface and the outer surface contributing to

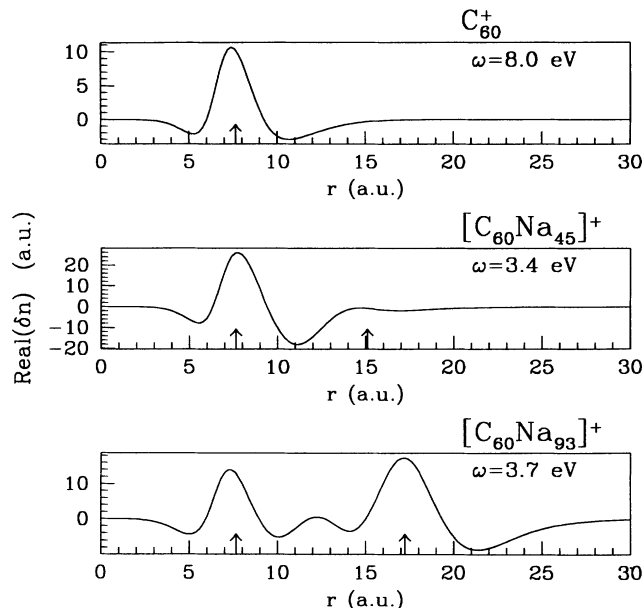


FIG. 5. Real part of the induced charge density corresponding to the collective mode frequency for C_{60}^+ , $[C_{60}Na_{45}]^+$ and $[C_{60}Na_{93}]^+$. Vertical arrows indicate the positions of the two interfaces (carbon-sodium and sodium-vacuum).

both resonances as we have. However, the plasmons are at different energies and we do not detect the classical two-peak structure in our results. The contrast between our results and the classical picture is similar to that found by Ekardt²⁹ in his study of the optical spectrum of coated metal clusters. The physical situation in the static limit, for which we have also performed calculations, is different. In this case, the induced density leading to the static dipole moment is located mainly at the sodium-vacuum interface for the coated clusters, with a well defined structure on the sodium adsorbate.

The inverse relation between polarizability and plasma resonance frequency [$\omega^2 \propto 1/\alpha(0)$] within classical models³³ suggests that the static polarizability may also provide some insight into the shift in dominant collective mode with Na coverage. In Fig. 6 the polarizability per electron is given as a function of the number of Na atoms coating the fullerene. We see a plateau for small coverages until $N \sim 13$, where the response of the coated cluster is dominated by the carbon which is much less polarizable than sodium. Then we observe an increase of $\alpha(0)$, which can be separated in two regions. Between $N=13$ and $N=21$ there is a qualitative change in the polarizability, which increases sharply. As N grows further the polarizability increases steadily towards the classical sodium limit, as the weight in the static response shifts from carbon to sodium. However, convergence to the large- N limit is slow,^{34,35} which is consistent with our previous finding that the carbon-sodium interface still has a role in the response for $N=93$, and higher coverage is needed to achieve Na-metal behavior. The sharp increase of $\alpha(0)$ with respect to the value for C_{60}^+ af-

ter $N \sim 13$ coincides with the occupation of electronic shells with principal quantum number $n = 2$, which extend further into the outermost region of the cluster than shells with $n = 1$ (see, for instance, the case $N=45$ in Fig. 2). After this sharp rise, the evolution of α is smoother and is associated with the progressive formation of a coating region with a density similar to that in metallic Na. However, a large number of Na atoms is needed for this region of “almost constant” electron density to fully develop. We observe a different behavior from that of metallic clusters where the polarizability per electron decreases (approximately as $N^{-1/3}$) as the size of the cluster increases.³⁶ Here the opposite trend results from the large polarizability of sodium as compared to carbon. We have only studied Na coverages leading to closed electronic shells; small oscillations of the polarizability for coverages intermediate between those plotted in Fig. 6 should be anticipated, but our study is enough to display the main trends in the optical response.

The slow convergence of the polarizability towards the classical value is typical of metallic aggregates. This slow convergence (from above) has been noticed in the experiments of Knight *et al.*³⁶ for the static polarizabilities of Na and K clusters, as well as in the experiments of Bréchnignac *et al.*³⁷ on the evolution of the surface plasmon resonance from a study of the photoabsorption cross section of large Li and K clusters. Those experiments show that the surface plasmon has not yet converged to the classical value even for clusters with one thousand atoms. We observe a similar slow convergence on the static polarizability (from below) for hollow clusters. This behavior is consistent with the size dependence of the classical polarizability of a hollow metallic sphere.³⁸

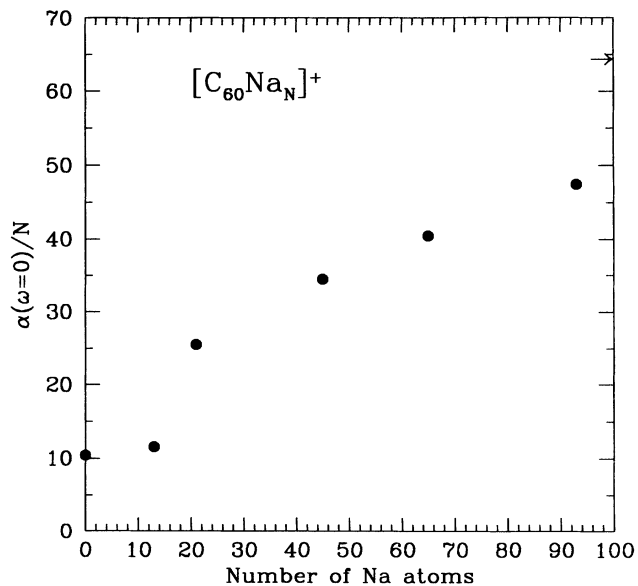


FIG. 6. Static polarizability per electron for $[C_{60}Na_N]^+$ clusters as a function of the number of Na atoms. The horizontal arrow indicates the classical limit for a spherical metallic sodium particle ($\alpha/N = 64$ a.u.³).

V. CONCLUSIONS

The two-shell model we have used to study ionized Na coated fullerenes ($[C_{60}Na_N]^+$) predicts a shift in response from a π -carbon collective mode to a metallic-Na excitation as the number of Na coating atoms is increased. A well developed excitation in the energy region of collective modes typical of pure Na clusters only occurs after the formation of an extended region with an electron density similar to that of metallic Na. However, the static polarizability is more sensitive to the presence of the coating and it sharply deviates from that of C_{60}^+ as early as for $N \sim 13$. The reliability of the method used has been confirmed previously in studies of the π plasmon in fullerenes, and we expect the present results to constitute a good description of the response properties of

coated fullerene clusters. Within our model similar optical dipolar properties are to be expected for Li, K, or Rb coverings, and, in general, for those metals for which the jellium model is justified. We hope that this work stimulates experimental investigations of the collective electronic excitations of these interesting systems.

ACKNOWLEDGMENTS

This work has been supported by DGICYT (Grants Nos. PB89-0352 and PB92-0645). One of us (A.R.) was supported by a Fulbright-MEC grant. M.J.S. acknowledges support from MEC (Spain) during his sabbatical stay in Valladolid. We acknowledge stimulating discussions with Professor L. C. Balbás.

* Permanent address: Departamento de Física Teórica, Universidad de Valladolid, Spain.

† Permanent address: Physics Department, Queen's University, Kingston, Ontario, Canada.

¹ H. W. Kroto, J. R. Heath, S. C. O'Brien, R. F. Curl, and R. E. Smalley, *Nature (London)* **318**, 162 (1985).

² W. Krätschmer, L. D. Lamb, K. Fostiropoulos, and D. R. Huffman, *Nature (London)* **347**, 354 (1990).

³ A. F. Hebard, M. J. Rosseinsky, R. C. Haddon, D. W. Murphy, S. H. Glarum, T. T. Palstra, A. P. Ramirez, and A. R. Kortan, *Nature (London)* **350**, 600 (1991).

⁴ T. P. Martin, U. Näher, H. Schaber, and U. Zimmermann, *Phys. Rev. Lett.* **70**, 3079 (1993).

⁵ O. Echt, K. Sattler, and E. Recknagel, *Phys. Rev. Lett.* **47**, 1121 (1981).

⁶ T. P. Martin, N. Malinowski, U. Zimmermann, U. Näher, and H. Schaber, *J. Chem. Phys.* **99**, 4210 (1993).

⁷ J. W. Keller and M. A. Coplan, *Chem. Phys. Lett.* **193**, 89 (1992).

⁸ A. A. Lucas, G. Gensterblum, J. J. Pireaux, P. A. Thiry, R. Caudano, J. P. Vigneron, Ph. Lambin, and W. Krätschmer, *Phys. Rev. B* **45**, 13 694 (1992).

⁹ G. F. Bertsch, A. Bulgac, D. Tománek, and Y. Wang, *Phys. Rev. Lett.* **67**, 2690 (1991).

¹⁰ G. Barton and G. Eberlin, *J. Chem. Phys.* **95**, 1512 (1991).

¹¹ A. Bulgac and M. Ju, *Phys. Rev. B* **46**, 4297 (1992).

¹² M. T. Michalewicz and M. P. Das, *Solid State Commun.* **84**, 1121 (1992).

¹³ A. Rubio, J. A. Alonso, J. M. López, and M. J. Stott, *Physica B* **183**, 247 (1993).

¹⁴ M. J. Puska and R. M. Nieminen, *Phys. Rev. A* **47**, 1181 (1993).

¹⁵ N. Van Giai and E. Lipparini, *Z. Phys.* **27**, 193 (1993).

¹⁶ D. Östling, P. Apell, and A. Rosén, *Europhys. Lett.* **21**, 539 (1993).

¹⁷ V. Kresin, *Phys. Rep.* **220**, 1 (1992).

¹⁸ J. A. Alonso and N. H. March, *Electrons in Metals and Alloys* (Academic, London, 1989).

¹⁹ A. Rubio, L. C. Balbás, and J. A. Alonso, *Phys. Rev. B* **45**, 13 657 (1992).

²⁰ J. M. Hawkins, A. Meyer, T. A. Lewis, S. Loren, and F. J. Hollander, *Science* **252**, 312 (1991).

²¹ W. Kohn and L. J. Sham, *Phys. Rev.* **140**, 1133 (1965).

²² W. Andreoni, P. Giannozzi, and M. Parrinello, *Phys. Rev. Lett.* **72**, 848 (1994).

²³ M. J. Stott and E. Zaremba, *Phys. Rev. A* **21**, 12 (1980).

²⁴ W. Ekardt, *Phys. Rev. Lett.* **52**, 1925 (1984).

²⁵ W. Ekardt, *Phys. Rev. B* **31**, 6360 (1985).

²⁶ A. Liebsch, *Phys. Rev. B* **36**, 7378 (1987).

²⁷ K. Nuroh, M. J. Stott, and E. Zaremba, *Phys. Rev. Lett.* **49**, 862 (1982).

²⁸ Z. Penzar, W. Ekardt, and A. Rubio, *Phys. Rev. B* **42**, 5040 (1990); J. M. Pacheco and R. A. Broglia, *Phys. Rev. Lett.* **62**, 1400 (1989).

²⁹ W. Ekardt, *Phys. Rev. B* **34**, 526 (1986).

³⁰ A. Liebsch, *Phys. Rev. Lett.* **67**, 2858 (1991).

³¹ J. M. Pacheco and W. Ekardt, *Ann. Phys. (Leipzig)* **1**, 252 (1992).

³² This confinement of the induced charge density at the interfaces has also been reported on experiments and random phase approximation calculations for bimetallic jellium films [see E. L. Yuh, E. G. Gwinn, P. R. Pinsukanjana, W. L. Schaich, P. F. Hopkins, and A. C. Gossard, *Phys. Rev. Lett.* **71**, 2126 (1993)]. These authors reported that the onset of the three dimensional surface film plasmon mode is very sensitive to the surface potentials and it is mode specific.

³³ A. A. Lushnikov, V. V. Maksimenko, and A. J. Simonov, in *Electromagnetic Surface Modes*, edited by A. D. Boardman (Wiley, New York, 1982), p. 305.

³⁴ A. Rubio and Ll. Serra, *Z. Phys. D* **26**, S118 (1993), and references therein.

³⁵ W. A. de Heer and W. A. Saunders, *Phys. Rev. B* **31**, 2539 (1985).

³⁶ W. Knight, K. Clemenger, W. A. de Heer, and W. A. Saunders, *Phys. Rev. B* **31**, 2539 (1985).

³⁷ C. Bréchnignac, Ph. Cahuzac, N. Kebaili, J. Leygnier, and A. Safarti, *Phys. Rev. Lett.* **68**, 3916 (1992).

³⁸ The ratio between the classical polarizabilities of two spheres with equal radius R_2 and dielectric constant ϵ , one of them with a central hole of radius R_1 is given by Ref. 29, $\alpha(\text{with hole})/\alpha(\text{no hole}) = (1 - q^3) \left[1 + \frac{2(1-\epsilon)^2 q^3}{(\epsilon+2)(1+2\epsilon)} \right]^{-1}$, where $q = R_1/R_2$. If we keep R_1 constant and increase R_2 , then $\alpha(\text{no hole})$ tends to its classical limit and the ratio $\alpha(\text{with hole})/\alpha(\text{no hole})$ tends to unity from below. On top of that, the quantum mechanical diffusiveness (spill out) of the electronic density leads to a slowing down of the convergence of $\alpha(\text{with hole})/\alpha(\text{no hole})$, in qualitative agreement with our results in Fig. 6.